

SAND98-1404C  
SAND-98-1404C

## Dilatometry in the Gleeble: What Did You Really Measure?

CONF-980657--

G. A. Knorovsky, C.V. Robino, R. C. Dykhuizen, D. O. MacCallum

Sandia National Laboratories  
Albuquerque, NM 87185

RECEIVED  
JUN 30 1998  
OSTI

### Abstract

The Gleeble<sup>®</sup> is an oft-used tool for welding metallurgy research. Besides producing synthetic weld specimens, it is used to determine phase transformation temperatures and kinetics via dilatometry. Experimental data and an FEM model are used to examine measured dilatation errors because of non-uniform heating of the dilatometer and other sources such as sample elastic and plastic deformation. Both isothermal and constant heating/cooling rate scenarios are considered. Further errors which may be introduced when the dilatation is incorrectly assumed to be linearly related to the volume fraction transformed are also discussed.

### Introduction

The Gleeble<sup>®</sup> is a sophisticated thermo-mechanical simulator used to produce specimens with a desired time-temperature-deformation history. It was originally invented[1] to produce 'bulk' samples simulating localized areas of weld heat affected zones (HAZ). Since the HAZ of a weld is characterized by steep gradients in peak temperature reached, HAZ microstructures may vary appreciably over short distances, making them hard to characterize, particularly with the tools available contemporary with the Gleeble's invention. Since that time, many new uses have been found such as simulation of rolling and forging, calorimetry, diffusion bonding, and apropos this work, studying the kinetics of solid-state reactions via dilatometry. Since most phase transformations involve some level of density change, measurement of specimen dimensions can be a sensitive probe of the extent of reaction. As always, there are complications in interpreting the data; we shall treat some of the commonly encountered (if not commonly recognized) errors inherent to dilatometry in this paper.

**Common Sources of Error:** Assuming good laboratory practice, proper personnel training and suitable equipment condition (calibration, functionality, and general repair), there are two major classes of non-uniformity that need to be addressed in the interpretation of any type of Gleeble test data. The first deals with material non-uniformity, while the second deals with thermal non-uniformity.

Examples of how material non-uniformity can impact Gleeble data include loose tolerance thermocouple wire leading to greater than expected temperature measurement error, and sampling error arising from inhomogeneous test material. For example, in non-cubic materials preferred orientation may affect the thermal expansion coefficient.

Thermal non-uniformity deals with two directions, transverse and longitudinal to the load application/current flow axis. The water-cooled jaws lead to the characteristic central hot zone in the Gleeble specimen, but less often recognized is the fact that the surface of the specimen, which is exposed to convective and radiative cooling (and conductive cooling from the local thermocouple and dilatometer contact points), can often be slightly cooler than the specimen core[2]. For precise temperature measurement work, these issues should be addressed, especially as the sample temperature exceeds red heat.

However, these are not the issues we wish to address; instead we will look at the commonly-made assumption that the dilatometer accurately measures the sample dilatation, and that the phase transformation fraction present at any given time may be linearly related to the distance from the extrapolated high and low temperature phase expansion curves.

**Dilatometer Resolution:** Our high resolution Gleeble diametral dilatometer is calibrated at 3.42 V/mm displacement; with its 12 bit, +/-10V range data acquisition system,  $(20 \text{ V} / 4096) = 0.00488 \text{ V}$  is the smallest voltage change resolvable, implying displacement resolution of 0.0014

\* Dynamic Systems Inc., Poestenkill, NY 12140

DISTRIBUTION OF THIS DOCUMENT IS UNLIMITED

MASTER

### **DISCLAIMER**

This report was prepared as an account of work sponsored by an agency of the United States Government. Neither the United States Government nor any agency thereof, nor any of their employees, makes any warranty, express or implied, or assumes any legal liability or responsibility for the accuracy, completeness, or usefulness of any information, apparatus, product, or process disclosed, or represents that its use would not infringe privately owned rights. Reference herein to any specific commercial product, process, or service by trade name, trademark, manufacturer, or otherwise does not necessarily constitute or imply its endorsement, recommendation, or favoring by the United States Government or any agency thereof. The views and opinions of authors expressed herein do not necessarily state or reflect those of the United States Government or any agency thereof.

## **DISCLAIMER**

**Portions of this document may be illegible electronic image products. Images are produced from the best available original document.**

mm (newer systems than ours will give a 10 V/mm calibration and attendant higher resolution). Given a 6.35 mm diameter (D) specimen, a fractional dilatation change of  $2.2 \times 10^{-4}$  is theoretically measurable. Relative density changes ( $\delta\rho$ ) of 1 to 5% for volume fraction changes ( $\delta V$ ) of 10 to 100% could be considered typical ranges which might be studied by this technique. Under ideal conditions, the dilatometric technique should be capable of detecting:  $\delta\rho/3 \times \delta V \times D = 2.2 \times 10^{-4}$ . If  $\delta\rho = 0.01$  and  $D = 6.35$ , the smallest  $\delta V$  detectable will be about 1% which is considered the minimal amount detectable by a variety of competitive techniques. Obviously, smaller/larger density differences will increase/decrease this threshold. Larger diameter specimens are also beneficial.

**Thermal Expansion of Dilatometer:** Since the dilatometer is in intimate thermal contact with the specimen, it heats up during testing. Because the high resolution Gleeble dilatometer suitable for phase transformation measurements is not symmetrical with respect to heating (the stationary arm is longer than the moveable arm and is 'L'-shaped) this adds an error term to the measured expansion. The high resolution dilatometer is not water-cooled; this may also add error due to changes in electrical response (not modeled here). For long duration tests we place a fiber heat shield between the transducer and specimen.

We became interested in whether this error term is appreciable, when some ~30 minute long isothermal hold transformation curves in an orthorhombic Ti-22Al-27Nb alloy showed an expansion at the highest transformation temperature and a contraction at lower temperatures (see Figure 1).

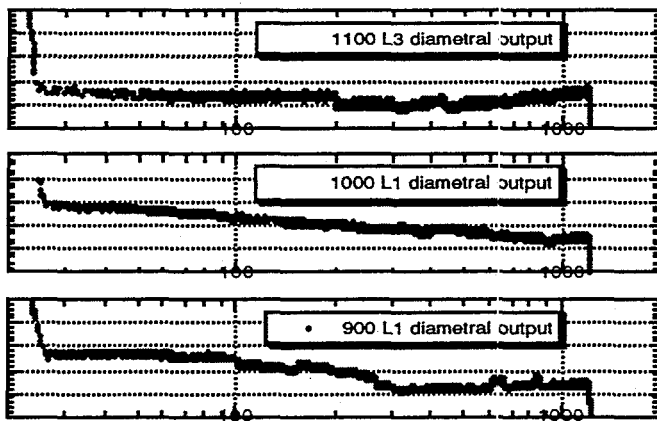


Figure 1: Dilatation (arbitrary units) vs hold time (s) of a Ti-22Al-27Nb alloy heated to a peak temperature of 1730°C, then cooled to the indicated temperature for a 20 minute isothermal hold showing unexpected change in behavior above 1000°C.

### Experimental Dilatation Data : Pure Ni

In order to simplify comparison between the model and experiment, we chose pure Nickel as a reference material; it is known to have no first order phase transformations in the temperature range of interest and reference data is readily available[3]. Two types of experiments were conducted:

continuous heating, and isothermal hold after a brief high temperature excursion. 6.35 mm diameter samples were run on a Gleeble Model 1500, using an environmental box which had been evacuated and then backfilled with argon. Type K thermocouples were used except for the peak/isothermal hold run, which required Type R.

Figure 2 shows the measured dilatation vs temperature curves obtained from pure Ni samples heated: 1) at 10°C/s to 650°C, then 0.1°C/s from 650 to 1000°C, 2) like 1) except at 1°C/s from 650 to 1000°C, 3) at 100°C/s to 1000°C from ambient; and 4) at 100°C/s to 1325°C from ambient, rapidly cooled to 975°C, held for 30 minutes. All samples were then free-cooled back to ambient. (The curves have been offset vertically to aid clarity; hereafter, condition 4 is referred to as the 'isothermal case'.) The rather unusual shapes of the rapidly changing temperature portions of the curves are due to undersampling and aliasing with electrical noise on the dilatometer output signal. In the slow-changing temperature portions of the curves many more data points were taken, and the error band is clearly discernible. This band can then be used to bound the expected errors on the sparsely-sampled portions. Agreement with the literature data on the dilatation of Ni [3], is satisfactory for the rapid heating/cooling dilatometer data; whereas the slow heating/cooling data do not agree as well. (The isothermal case curve shows additional anomalous behavior which will be discussed later.)

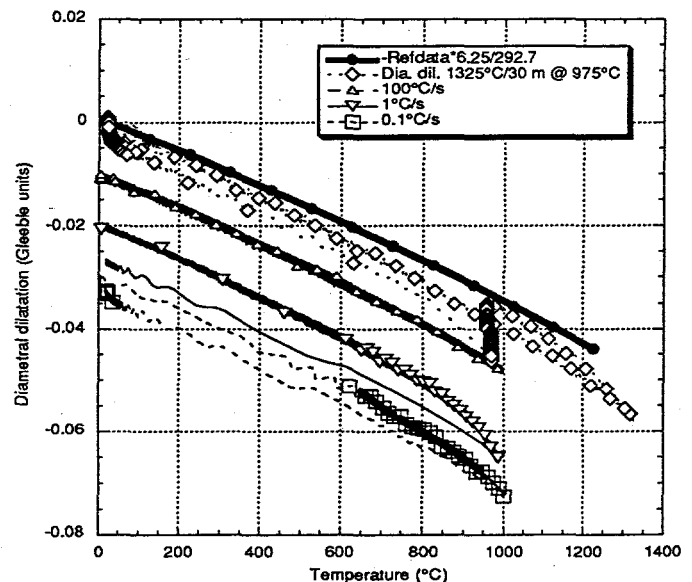


Figure 2: Dilatation vs Temperature as a function of thermal cycle (see text) for 6.35 mm diameter specimens of pure Ni. Multiply Gleeble units by 2.927 to get mm.

### Dilatometer Model

Using COSMOS/M\* finite element software, a simple

\* Structural Research and Analysis Corp. Los Angeles, CA, 90025-1170

2D model of the Gleeble high resolution dilatometer was built; it required 175 nodes and 113 elements. The mesh used, and the boundary conditions are shown in Figure 3, where the round specimen is of 6.35 mm diameter.

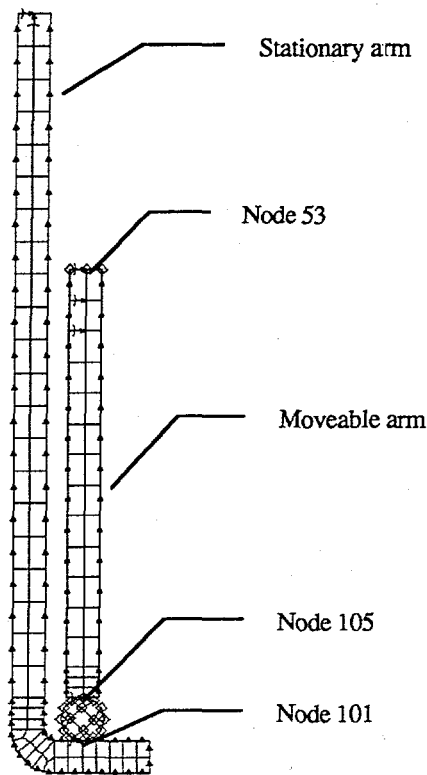


Figure 3: Mesh and boundary conditions for the model. Triangles are convective boundary conditions (bc's), diamonds are temperature bc's, arrows are displacement bc's, rectangles are individual elements. Nodes are not illustrated, but occur at the corners of the 4-node elements. Specimen diameter = 6.35mm.

The intent of the model was to determine if the differential heating of the two arms would lead to appreciable error. The model incorporated available data on fused silica for conductivity, density, heat capacity, and coefficient of thermal expansion (CTE)[4]; these values were assumed constant vs temperature. Perfect thermal contact at the arm/specimen interface nodes (node 101: stationary arm/specimen & node 105:moveable arm/specimen) was assumed, and convective cooling to room temperature air along the surface of the dilatometer shafts was incorporated. Radiational heating/cooling was not used. The specimen was simulated as having the room temperature thermal properties of pure Ni, (except that an essentially zero value for CTE was used for some calculations to make all displacement due to the arm expansion), and given uniform temperature vs time histories to match experiment. The 'L'-shaped stationary arm of the dilatometer was pinned against rectilinear displacement at its top end, while nodes 101 and 105 were constrained to move vertically, as was the top end of the moveable arm (node 53). The top end of the moveable arm was constrained to ambient temperature (on the actual dilatometer,

this contacts an Al sleeve). We then calculated the thermoelastically-induced displacement at the top and bottom of the specimen (node 105 & node 101, respectively), and the top of the moveable arm (node 53) under simulated thermal cycling. The actual dilatation of the sample is the difference in displacement between nodes 101 and 105 (and is zero when the specimen CTE is set to zero). The displacement of node 53 is what the dilatometer transducer measures.

**Continuous Heating Rate Cases:** As noted above, in most calculations the Ni specimen was given a zero expansion coefficient; thus, the node 101 and node 105 data superimpose, and the displacements plotted are solely due to the thermal expansion of the dilatometer arms.

The 100°C/s heating rate (Figure 4) gives very little time for heat transfer to occur, so the calculated behavior of the dilatometer is quite good; the maximum error in apparent dilatation (the absolute value of node 53's displacement = 0.0015 mm) about equals the detection limit of the system (0.0014 mm). Node 101's motion is smaller, and delayed in time.

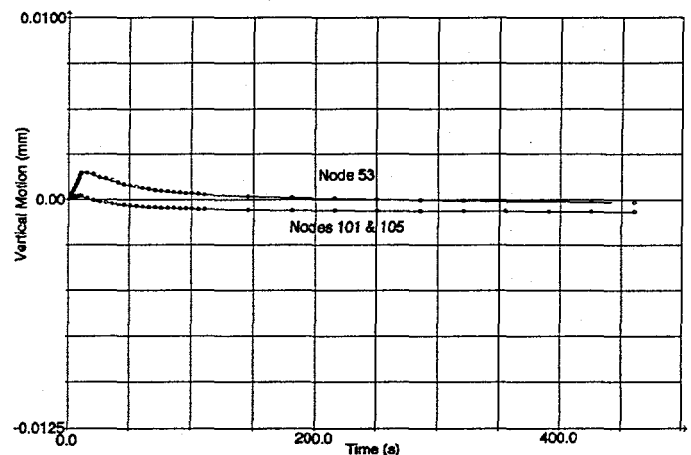


Figure 4: Heated at 100°C/s to 1000°C; zero CTE for Ni.

At a heating rate of 1°C/s (Figure 5) appreciable negative motion for nodes 101 & 105 occurs, implying significant heating of the stationary arm. Similarly, node 53 moves in a positive direction an equal magnitude, implying expansion of the moveable arm as well. Furthermore, the maximum error is about three times larger (~.0041 mm), and continues to increase until the sample begins cooling. This error is about three times the detectability limit.

For the sample heated at 0.1°C/s between 650 and 1000°C calculations with both the actual (Figure 6) and zero (Figure 7) CTE for Ni were made. (Note Figure 6's vertical scale is 10x larger than previous plots.) The relative arm/sample displacements can be compared between the two figures. The calculated apparent dilatation from ambient to 1000°C is 0.14 mm, compared with 0.13 mm obtainable from Figure 2. The actual sample dilatation is the difference between nodes 101 and 105, so the difference between 105 and 53 is not all error. Figure 7 shows that dilatometer error behavior similar to the 1°C/s case

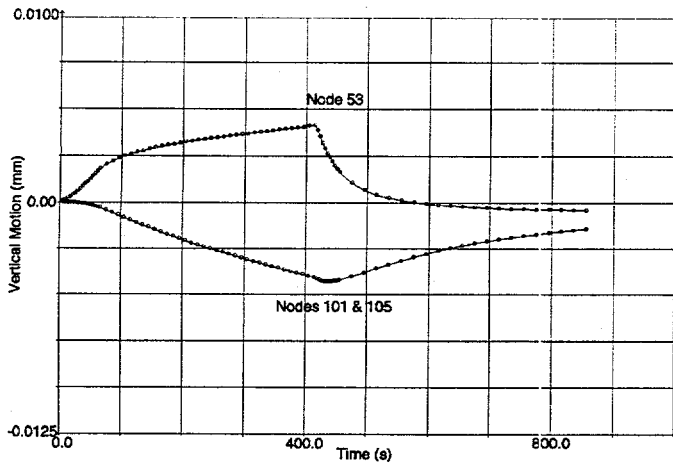


Figure 5: Heated at 1°C/s between 650 and 1000°C; zero CTE used for Ni.

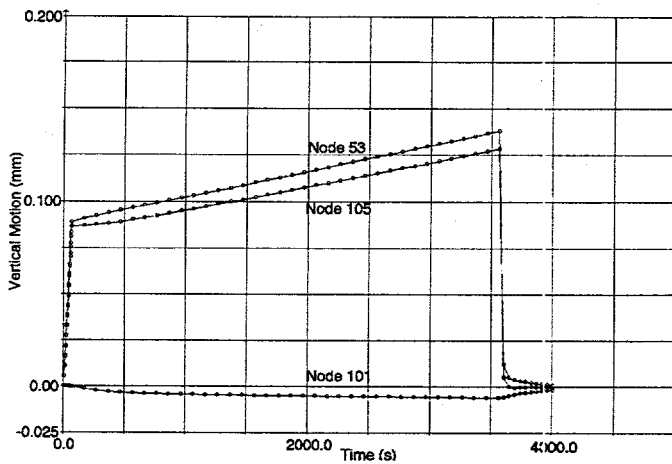


Figure 6: Heated at 0.1°C/s between 650 and 1000°C; Ni CTE.

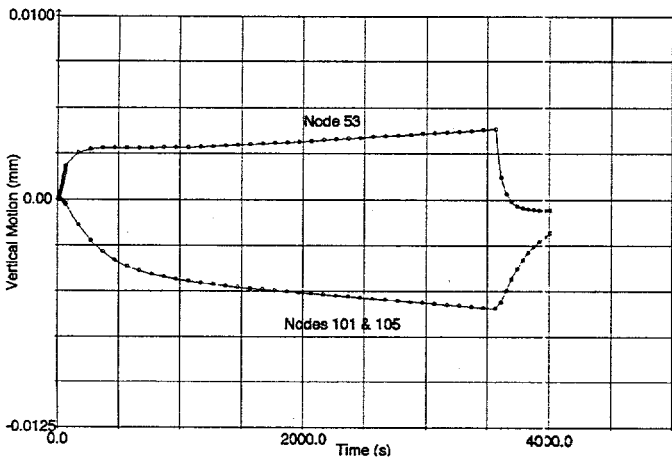


Figure 7: Heated at 0.1°C/s between 650 and 1000°C; zero CTE used for Ni.

is again obtained (note 5x horizontal scale relative to Figure 5). Note that the overall error is actually slightly smaller for the 0.1°C/s case than the 1°C/s case, in qualitative agreement with the deviations from reference data in Figure 2.

**Isothermal Case:** During the isothermal hold (Figure 8), an apparent expansion is calculated to occur when none is actually present, in qualitative agreement with the data of Figure 2. The error increases relatively quickly to its maximum, taking about 2 minutes. The calculated maximum magnitude of the error, ~0.0043 mm is about 3x that seen for the 100°C/s continuous heating case, essentially the same as the 1°C/s and 0.1°C/s cases. However, in those previous cases the error was increasing with time; here it decreases after reaching a maximum. Note also, that the motion of the stationary arm specimen contact point is again of the same magnitude but opposite sense to that of the moveable arm, implying that the

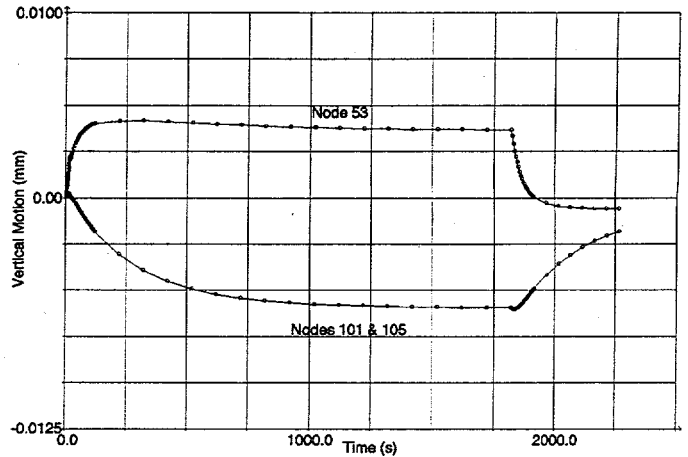


Figure 8: Rapidly heated to 1325°C, then cooled and held isothermally at 980°C for 30 minutes; zero CTE used for Ni.

latter's total expansion (the difference between the curves) is about twice as much. Again, the moveable arm reaches equilibrium somewhat sooner than the stationary arm.

**Comparison between model and experiment:**

In Figure 2 the apparent displacement measured during the isothermal case's hold is ~ 0.03 mm, nearly an order of magnitude greater than calculated; furthermore it does not decrease toward the end of the hold period. However, the data is somewhat anomalous in that the endpoints of the isothermal hold displacement data do not fall on either the original on-heating curve from room temperature, or the upward extrapolation of the final transient on-cooling to ambient. Other replicates gave similar values, and also showed the increased slope at temperatures > 1200°C.

For the continuous heating experiments, if one examines the deviation from the Ni reference data for the 0.1°C/s data, it is found to be 0.015 mm. The calculated error value was 0.0038 mm. For the 1°C/s data, the measured deviation was 0.022 mm, where the calculated value was 0.004 mm. For the 100°C/s data, the deviation is 0.0008 mm, the calculated value 0.0015 mm. Based upon these comparisons, it appears that the component of error due to differential thermal expansion of the dilatometer arms is only a small part of the discrepancy. However, detection of the transformation start is an important role of dilatometry. It is possible that this error source could be important if it overlaps the transformation start.

We employed a temperature bc at the sample/dilatometer contact nodes because heat transfer physics across contact interfaces was beyond the scope of this simple model. To examine this assumption, we ran cases where the dilatometer surface nodes horizontally adjacent to nodes 101 and 105 had identical temperature bc's. Heat transfer to both arms increased, as shown by increased motion of nodes 101 & 105. However, these motions offset and node 53 motion slightly decreased. If the bc was applied to all the end nodes of the moving arm and just the contact node of the stationary arm (to maximize heat flow asymmetry) an increase in node 53 motion (~20%) was seen relative to the original bc's. While not changing our conclusions, these calculations suggest that surface condition of the dilatometer arms can affect the measurements.

**Additional error due to deformation:** Another error complicating the interpretation of Gleeble dilatation data involves plastic deformation of the specimen due to frictional loading of the actuator rod by the environmental chamber seals. In this case, the expansion and contraction of the sample is resisted by the actuator rod seal friction. At sufficiently elevated temperatures this force (measured as  $\leq 1000$  N) can deform many materials, including pure Ni. We believe this explains the high temperature behavior of the isothermal run where the slope of the dilatation increases at  $\sim 1200^\circ\text{C}$  on heating and on cooling from the peak temperature. If one assumes that the material's flow stress is exceeded at elevated temperatures by the frictional forces, all the longitudinal thermal strain that should occur is converted into transverse plastic strain. This strain, added to the normal thermal expansion strain can be shown to increase the dilatation vs temperature slope according to the equation:

$$\Delta d(\text{dilatation})/dT = (1 + \text{freespan}/(3 \times \text{effective gauge length}))$$

A freespan/gauge length ratio of 6 completely explains the maximum increase in slope seen in our isothermal case specimens. The freespan for our samples was 30 mm. The gauge length might be expected to be on the order of the sample diameter (6.35 mm), so a ratio of 6 is not unreasonable. Furthermore, the increased slope relative to the Ni reference dilatation data noted on cooling from the isothermal hold (in the  $800\text{--}1000^\circ\text{C}$  temperature region) can be explained by assuming the sample is transitioning from a condition of compression to tensile yield. Instead of the transverse strain factor of 0.5 which is built into the equation noted above (from the assumption of zero volume change on plastic deformation), Poisson's ratio ( $\sim 0.3$ ) should be used. This reduces the term added to 1 inside the parenthesis, and gives a slope enhancement of about 0.6 the value seen for the plastic strain case. The actual value of the slope ratio was found to be 0.67. The remaining discrepancy may be explained by a slightly narrower gauge length on-cooling relative to on-heating (the steeper dilatation vs temperature slope for on cooling was also seen in the plastic flow case).

By using a low-force load cell inside the environmental chamber, and force control mode, this source of error should be reduced or eliminated. Verification experiments are planned. Given the above analysis, creep is a likely mechanism to explain the apparent expansion during the isothermal hold.

## Determining Fraction Transformed from Dilatation Data

During a phase transformation, the distribution and amounts of phases present change. When the reaction is complete, depending upon the type of transformation, the final density of the sample may be uniform or not, but the measured final apparent density will be an average of the local density distribution. When using dilatation data to determine fraction transformed it is common to make the assumption that the progress of the transformation is linearly related to the instantaneous value of dilatation change normalized by the overall dilatation change (for isothermal transformations). When non-isothermal reactions are being studied, the fraction transformed is taken as the fractional distance of the dilatation curve between the extrapolated low and high temperature phase dilatation curves plotted vs temperature. As we shall see, these assumptions can give very poor results.

In general:  $\rho_{\text{app}} = \sum_i V_i \rho_i$  where  $V_i$  = volume fraction of phase  $i$  (summation of  $i$  is over all phases) and for each phase  $i$ :  $\rho_i = \rho_i(\text{composition, temperature})$ , and  $V_i = V_i(\text{composition, temperature, time})$ .  $V_i$  of each phase  $i$  is desired as a function of time, given that  $\rho_{\text{app}}$  has been measured as a function of time.  $\sum_i V_i = 1$ , and information from the equilibrium phase diagram relating temperatures and compositions for individual phases and aggregates of phases is assumed available. Overall:

$$d\rho_{\text{app}} = d(\sum_i V_i \rho_i) = \sum_i (V_i d\rho_i + \rho_i dV_i)$$

however, since:

$$d\rho_i = (\partial\rho_i/\partial c)dc + (\partial\rho_i/\partial T)dT \text{ and} \\ dV_i = (\partial V_i/\partial c)dc + (\partial V_i/\partial T)dT + (\partial V_i/\partial t)dt$$

by substituting, we arrive at:

$$d\rho_{\text{app}} = \sum_i [V_i \{ (\partial\rho_i/\partial c)dc + (\partial\rho_i/\partial T)dT \} + \rho_i \{ (\partial V_i/\partial c)dc + (\partial V_i/\partial T)dT + (\partial V_i/\partial t)dt \}]$$

Assuming that we know the time vs temperature behavior (i.e.  $T = f(t)$  and  $dT/dt = f'$ ), and since the compositions of phases vs temperature are known from the phase diagram (i.e.  $c = k(T)$  and  $dc/dT = k'$ ), we can then transform the previous equation into a function of time:

$$d\rho_{\text{app}} = \sum_i [V_i \{ (\partial\rho_i/\partial c)k'f' dt + (\partial\rho_i/\partial T)f' dt \} + \rho_i \{ (\partial V_i/\partial c)k'f' dt + (\partial V_i/\partial T)f' dt + (\partial V_i/\partial t)dt \}]$$

In the case of a pure material undergoing an isothermal allotropic phase change, while there will be two phases present, all terms involving partial derivatives taken with respect to temperature or composition are zero, simplifying the above equation to:

$$d\rho_{\text{app}} = (\rho_1 - \rho_2)dV_1$$

Thus, the fraction transformed is directly related to the measured density change by the difference between the high and low temperature phase densities. If however, the temperature is not held constant (but is still uniform in the sample, and assuming

that  $V_i$  is not affected by  $T$ , i.e. the reaction goes to completion if it occurs at all):

$$d\rho_{app} = [V_1(\partial\rho_1/\partial T) + (1-V_1)(\partial\rho_2/\partial T)]f'dt + (\rho_1 - \rho_2)dV_1$$

and while correction terms are needed due to the the phase densities changing with temperature, the fraction transformed is still fairly easy to obtain. In the case where three phases are present, such as the austenite-ferrite-cementite eutectoid reaction in Fe-C, we have at the invariant:

$$d\rho_{app} = (\rho_f - \rho_a)dV_f/dt + (\rho_c - \rho_a)dV_c/dt$$

At the invariant, the ratios of  $dV_a/dt / dV_c/dt$  and  $dV_a/dt / dV_f/dt$  will be given by the lever rule. Since the density differences between the ferrite, austenite, and cementite are known, we can relate the dilatation to the phase fraction changes. However, as soon as we allow phase densities to vary with position by moving away from the invariant point (introducing both non-uniform temperature and composition), previously zeroed partial differential correction terms re-enter, and in general further assumptions are needed in order to obtain a unique set of phase fractions. Additionally, the summation should be replaced with an integral equation. Onink et.al [5] have analyzed the case for the decomposition of austenite to ferrite-pearlite aggregates, whereas Dykhuizen et.al [6] have analyzed the reverse reaction. In both cases, assumptions are made about the progress of the transformation to take into account the non-uniformity of composition associated with position and temperature. Figure 9 from Dykhuizen et.al., shows that the simple assumption of linear conversion of the dilatation data instead of a more physically realistic model can lead to a dramatically different data interpretation.

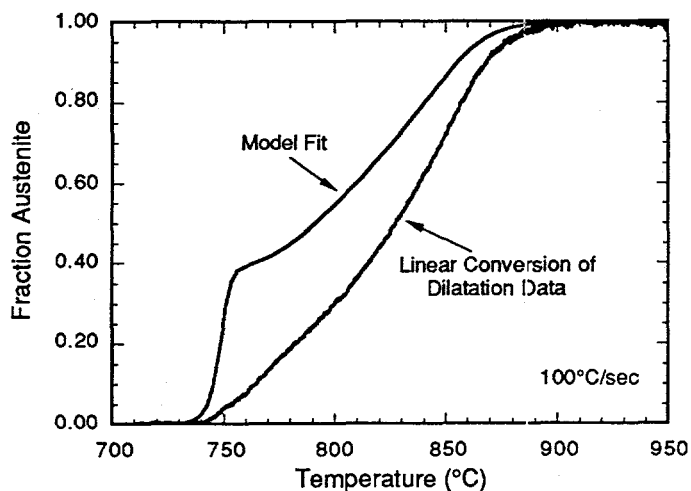


Figure 9: Difference in fraction transformed determined from dilatation: linear assumption vs physically-realistic model, austenitization of pearlitic structure in 0.29wt% C steel [6].

### Conclusions

Discrepancies noted in the use of dilatation measurements to determine phase transformation kinetics led to

an investigation of possible sources of error. Most notably, isothermal holds on stable specimens (pure Ni) gave an apparent dilatation increase with time. Using a simple 2D finite element model to calculate the error caused by asymmetric heating of dilatometer arms we concluded that this source explained only a small part of the behavior seen in the Ni experiments whether for isothermal or continuously heated thermal cycles, but could be a significant source of error when transformation start times are sought. In order to eliminate such errors from phase transformation data, careful calibration experiments to establish a baseline using similar but stable specimens should be run. Furthermore, we pointed out two other pitfalls to interpretation of dilatation data, namely, non-linearity of apparent dilatation and fraction transformed and environmental chamber seal frictional loading-induced deformation. The frictional loading explanation implicates plastic deformation and creep as being the most likely source of the apparent isothermal dilatation increase seen in Ni. The Gleeble is a powerful tool for metallurgical research; however, its outputs need to be carefully analyzed before accurate data can be obtained.

### Acknowledgments

This work was supported by the United States Department of Energy under Contract DE-AC04-94AL85000. Sandia is a multiprogram laboratory operated by Sandia Corporation, a Lockheed Martin Company, for the United States Department of Energy.

### Bibliography

- 1 E.F. Nippes, W.F. Savage, B.T. Bastin, H.F. Mason, R.M. Curran, 'An Investigation of the Hot Ductility of High Temperature Alloys', *Welding Journal Res. Suppl.*, 34(4), pp 183-196s, (1955).
- 2 Personal communication with Dave Jacon, DSI, Poestenkill, NY, DSI-provided reports: "Measurement of Radial Gradients: Tubular Specimen Disappearing Wall Method" and "Measurement Errors: Radial Gradients in Slotted Specimens", no authors given, May, 1998.
- 3 Y.S. Touloukian, *Thermophysical Properties of Matter*, IFWPlenum, New York, (1975).
- 4 W.H.Kohl, *Handbook of Materials and Techniques for Vacuum Devices*, Reinhold Publishing Co, New York, (1967).
- 5 M. Onink, F.D. Tichelaar, C.M. Brakman, E.J. Mittermeijer, S. van der Zwaag, 'Quantitative Analysis of the Dilatation by Decomposition of Fe-C Austenites; Calculation of Volume Change upon Transformation', *Z. Metallkunde*, 87, pp 24-32, (1996).
- 6 R.C. Dykhuizen, C.V. Robino, G.A. Knorovsky, 'A Method for Extracting Phase Change Kinetics from Dilatation for Multi-Step Transformation: Austenitization of a Low Carbon Steel', submitted to *Metallurgical and Materials Transactions B*, April, 1998.